



Luminescence Saturation in Inorganic Phosphors under High Flux of Photon Excitation

Yong Nam Ahn, Hyun Woo Park, Tae Gil Lim, and Jae Soo Yoo  ^z

School of Chemical Engineering and Materials Science, Chung-Ang University, Dongjak-gu, Seoul 06974, Korea

The luminescence behavior of certain phosphor material shows non-linearity within a specific photon excitation range, depending upon the activator and/or the host lattice. Conventionally, the absorption and emission characteristics of phosphors are measured using a spectrometer with a light source such as a xenon lamp. Herein, a new measurement system was set up to investigate luminescence saturation in inorganic phosphors. The effect of the environment on the longevity of the material has been examined for each attribute and the conditions for luminescence saturation have been discussed.

© The Author(s) 2018. Published by ECS. This is an open access article distributed under the terms of the Creative Commons Attribution Non-Commercial No Derivatives 4.0 License (CC BY-NC-ND, <http://creativecommons.org/licenses/by-nc-nd/4.0/>), which permits non-commercial reuse, distribution, and reproduction in any medium, provided the original work is not changed in any way and is properly cited. For permission for commercial reuse, please email: oa@electrochem.org. [DOI: 10.1149/2.0291806jss]



Manuscript submitted April 5, 2018; revised manuscript received May 30, 2018. Published June 19, 2018.

Phosphor-converted white light-emitting diodes (pc-WLEDs) are widely used as a light source in liquid crystal displays and in solid-state lighting. They are known to be more stable than Ne-, fluorescent-, and halogen-lamps. In addition, they exhibit an excellent efficiency of ~ 246 lm/W at 20 mA. The pc-WLEDs directly convert electrical energy into light.¹⁻⁴ In this conversion process, some electrical energy is dissipated in the form of heat, which leads to a decrease in the light efficiency. Heat sinks and cooling fans are also sources of LED power consumption that lead to a non-negligible decline in the lighting efficiency.^{5,6}

As the applications of high-power pc-WLEDs continue to increase, ensuring the reliability of these devices in terms of their optical characteristics and thermal stability has gained importance. In particular, a decrease in the efficiency of the power output and life-time has also been reported.^{7,8} As the current density of the pc-WLEDs increases, their light output also increases and more heat is emitted.⁹⁻¹¹ It is known that the heat generated in the device increases the temperature of the active region of the quantum-well (QW) layer in the LED structure. The elevated temperature may also decrease the bandgap of the active region, which would cause the generation of more heat due to non-radiative recombination in the active region. This positive feedback process reduces the quantum efficiency of the LED and eventually causes degradation of its luminance and lifetime.¹²

However, a more commonly encountered phenomenon is droop, in which the efficiency decreases over a certain level as the output increases. Although many studies have focused on clarifying the cause of the droop phenomenon and implicated sources such as carrier heating, carrier escape, and the Auger effect, the exact cause has not been identified as yet.¹³⁻¹⁶ Therefore, further detailed studies are necessary.

In general, the reliability of pc-WLEDs at high light-output emission is evaluated by using a LED package consisting of a blue-emitting LED chip and inorganic phosphors such as $Y_3Al_5O_{12}:Ce^{3+}$ (YAG) and $K_2SiF_6:Mn^{4+}$ (KSF), etc.^{9,17-19} Under high light-emission, more heat is generated in the process of converting electrical energy into light because of the droop phenomenon of the LED chip itself and the increase in the emission wavelength or a shift in the wavelength depending on the physical characteristics of the phosphor, such as thermal stability. This, in turn, lowers the light efficiency of the doped inorganic phosphor.^{5,20}

Therefore, the reliability of the LED package must be examined with a focus on the material comprising the doped inorganic phosphor as well as the droop phenomenon. It is also time-consuming to evaluate the optical durability and thermal stability of inorganic phosphors using the existing evaluation equipment such as LM-80 because of the constraints of this system.

However, laser diodes (LDs) have high efficiency, are similar to LEDs, and exhibit higher light output under stimulated emission.²¹ In addition, the light quality is much superior to that of LEDs with a narrower bandwidth. Moreover, the photo-emission of LDs is linearly correlated with the injected current density. Therefore, LDs can function as an excellent light source for LED pumping, where the droop phenomenon can be relaxed. Hence, LDs are used as a light source for the aforementioned analysis.²²⁻²⁴

Herein, a new and reliable evaluation system for analyzing the optical durability and thermal stability of inorganic phosphors has been developed. Using this protocol, the performance of a phosphor under high intensity excitation was evaluated, which afforded high intensity photo-excitation and did not cause the droop phenomenon. Moreover, the important issue of "luminescence saturation" has also been investigated as a phenomenon in which the efficiency of the phosphor decreases at very high flux of photon excitation. Under high flux of photon excitation, the relationship of luminescence saturation to material properties is discussed.

Experimental

The equipment, as shown in Fig. 1, was constructed to evaluate the high-speed reliability of the phosphor, in high speed as a solid phase powder itself. This equipment is used to measure the optical durability of phosphors with the excitation source of LED/LD (Laser Diode) at high optical density. The reliability evaluation system was composed of the light source, a sample holder, a light detector, an integrating sphere to prevent leakage of the reflected light to the incident light source, an optical fiber and a cutoff filter that differentiated between the light originating from the light source and emitted light. The incident light source could be operated in either continuous wave (CW) mode and/or pulsed mode to avoid self-heating. Since we built our own equipment, we evaluated the stability of LD and the fact that the efficiency does not deteriorate even at high power.

In Fig. 2, the performance of a 450nm-emitting LD, which is mounted on the equipment, was evaluated. Here, the spot size on the target by an LD is kept constant by keeping the distance between the target and an LD close as much as possible. Repeated measurements were made at room temperature and air, not under N_2 atmosphere, to ensure the reliability of our equipment. The relative photon density was confirmed, as depicted in Fig. 2. As shown in Fig. 1, $BaSO_4$ was applied to the sample holder placed on the Peltier to totally reflect the wavelength of 450m excited from the LD. The excited LD is all reflected by $BaSO_4$ and likewise reflected by doped $BaSO_4$ inside the integrating sphere. The reflected light is transmitted to the detector through the optical fiber, and the result is shown in Fig. 2. In this scheme, the size of beam spot is less than 1.12 mm diameter. However, the photon intensity on the target is relatively quantized. To verify the number of maximum acceptable photons (N_{MAP}) for each phosphor, a

^zE-mail: jsyoo@cau.ac.kr

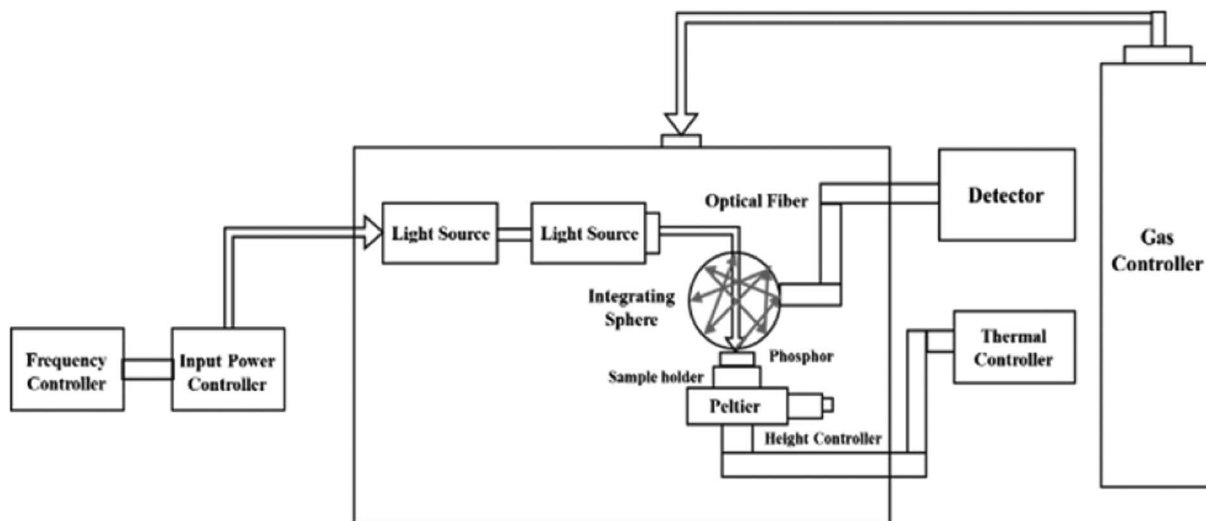
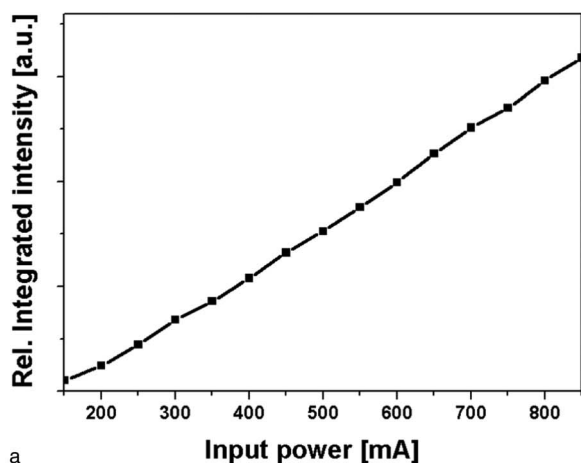
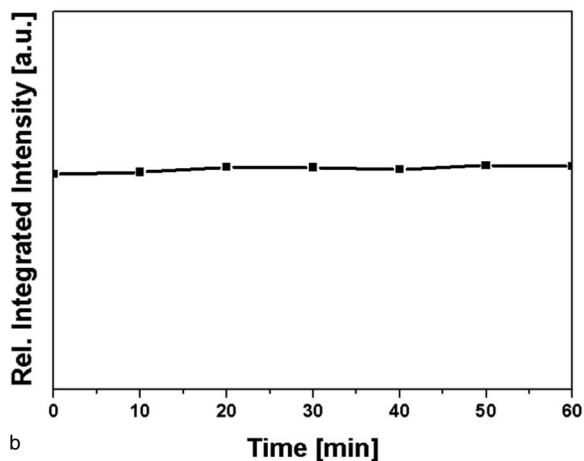


Figure 1. Schematic diagram of high-speed reliability evaluation system.

commercial level of YAG was applied to the sample holder to account for this as a photon-saturation phenomenon. The YAG was measured by increasing the intensity of the light source by 50mA from 200mA which is the reference point of the output.



a



b

Figure 2. a. Linearity of the photons output on the driving current of a laser diode (LD) used in this experiment. No saturation is observed within our experimental regime. The beam spot size is 1.12 mm of a diameter. b. Stability of the LD over time at a high power operation of 550mA in CW mode.

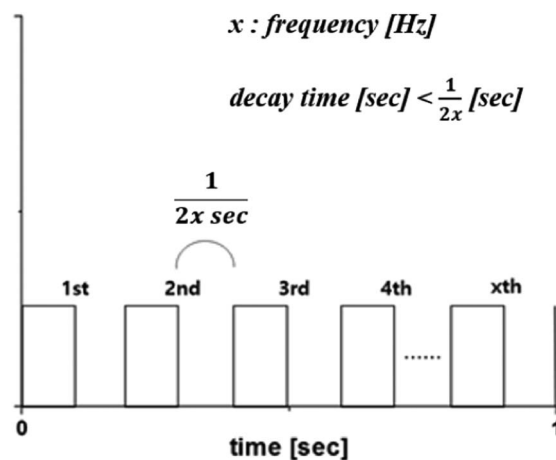


Figure 3. Pulse frequency for deriving the LD. It is determined based upon the decay time of phosphor to avoid the effect of photon accumulation on the phosphor.

In addition, to clearly distinguish the effects of self-heating of non-radiative recombination, the YAG was measured in CW mode and pulsed mode, respectively.^{22,25} Light source irradiated in pulsed mode was excited with a frequency of 3.57 Hz to prevent photons from accumulating due to long decay time and thereby self-heating, as shown in Fig. 3.

Dependence of the temperature on the luminescence saturation was also evaluated. We compared the temperature-dependency on the luminescence saturation in the interval from 298K to 423K. Finally, it is demonstrated that the luminescence saturation is a result of an excessive number of photons and not because of the decrease in efficiency due to the destruction of the crystal structure by checking the reversibility of luminescence behavior at high flux of photon excitation.

Results and Discussion

Luminescence saturation was observed for the inorganic compounds at a high flux of photon excitation. Here, we have defined the observed degradation as “luminescence saturation”. This phenomenon means that as the current applied to the light source increases, the optical characteristics increase, but the photons accumulated at a certain density or more are saturated finally, resulting in a drastic decrease

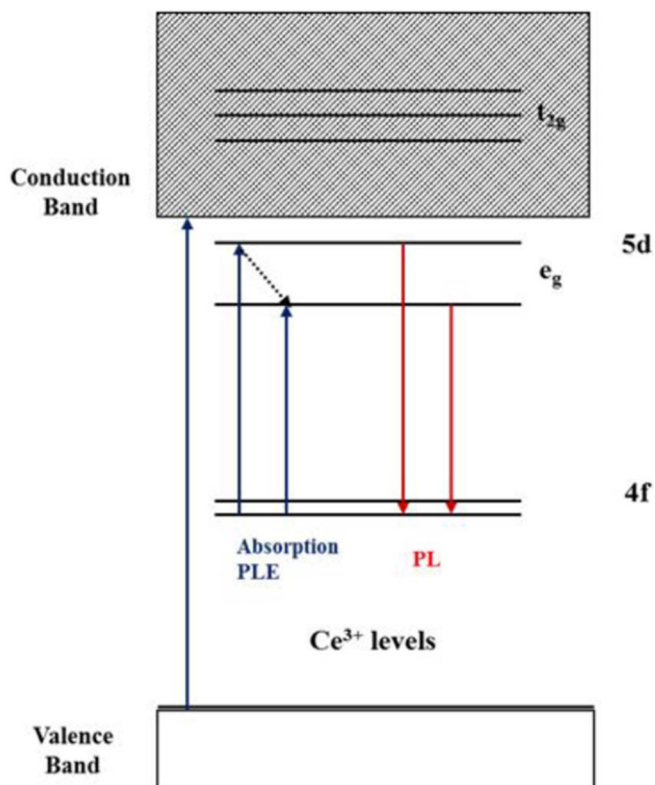


Figure 4. Energy transition in $Y_3Al_5O_{12}:Ce^{3+}$ by photoluminescence.

in the light efficiency. This is illustrated by following equations.

$$N_{exc} \cdot Abs \cdot P_{GE} \cdot (1 - P_{EG}) \cdot \frac{A_s}{A} \cdot \tau(T) \cdot c \geq N_{MAP} \quad [1]$$

$$N_{accum} = N_{exc} \cdot Abs \cdot P_{GE} \cdot (1 - P_{EG}) = \int \frac{dN_{in}}{dt} - \int \frac{dN_{out}}{dt}$$

when

$$\frac{dN_{out}}{dt} < \frac{dN_{in}}{dt} \quad [2]$$

$$N_{accum} = 0$$

when

$$\frac{dN_{out}}{dt} \geq \frac{dN_{in}}{dt} \quad [3]$$

The N_{MAP} indicates the maximum number of acceptable photons and is an inherent, unique characteristic for each phosphor. N_{exc} indicates the number of photons supplied by the LD output, Abs is the degree of absorption of the light source, and P_{GE} and P_{EG} indicate the probability of the system being excited from the ground state to the excited state and returning from the excited state to the ground state, respectively. Here, $\tau(T)$ is a function of the temperature and indicates the effective decay time, A is the area of the laser source, and A_s is the area of the laser spot. Also, c is a constant that compensates for the effects of temperature and corrects the decay time and release rate.

In Fig. 4, the energy transitions in YAG under photoexcitation is expressed.²⁶ The electronic configuration of Ce^{3+} ion is $[Xe]4f^1$, and the energy gap between the lowest 5d orbital and 4f ground state is large. The ground state is split into $^2F_{5/2}$ and $^2F_{7/2}$ by spin-orbit interaction. In addition, the 5d configuration of the Ce^{3+} ion combined with the host lattice ($Y_3Al_5O_{12}$) is split by the crystal field into a doublet (e_g) with lower energy and a triplet (t_{2g}) with higher

energy. The excitation absorbed by the phosphor is excited from the $4f^1(^2F_{7/2})$ to $4f^05d^1$ excited state, and the excited photons are emitted in the form of light and heat, respectively, with radiative recombination and non-radiative recombination.²⁷⁻³⁰ According to the energy transitions above, the photons absorbed from the LD are excited from the $4f^1(^2F_{7/2})$ ground state to $4f^05d^1$ excited state and the excited photons are then relaxed to the $4f^1(^2F_{7/2})$ ground state. The relaxation is divided into two types: non-radiative recombination (dotted line in Fig. 4) and radiative recombination (downward red vertical arrow in Fig. 4).²⁵

In this process, there occurs a difference in the velocity of photons (or number) excited and the velocity of photons (or number) emitted, so that a relaxation process cannot be performed to the $4f^1(^2F_{7/2})$ ground state and accumulation occurs in the $4f^05d^1$ excited state. Luminescence saturation means that the optical efficiency drops when the number of accumulated photons (N_{accum}) exceeds the intrinsic N_{MAP} of the phosphor, or when the number of photons excited by the $4f^05d^1$ excited state exceeds the N_{MAP} . Thus, when the left and the right sides of Eq. 1 have the same value, the photon can no longer fall to the ground state, and this point is called the "saturation point". It is the point in time when the number of photons entering the excited state. In this case, N_{accum} can be obtained as shown in Eqs. 2 and 3, according to these two cases. When the velocity of photon absorption exceeds that of photon emission, photon accumulation starts to occur and the N_{accum} is the integral of the difference between the velocities of N_{in} ($= N_{exc} \cdot Abs \cdot P_{GE}$) and N_{out} ($= N_{in} \cdot P_{EG}$). When the velocity of N_{out} is faster than that of N_{accum} is zero. This is because all the photons are emitted in the form of light or heat through the relaxation process. When N_{MAP} is equal to N_{accum} , photon saturation begins to occur.

As depicted in Fig. 5, the photoluminescence spectra of YAG as current applied to the LD irradiated in the CW mode increases and the integrated value of the intensities of the emission wavelength (480~720nm) with LD-driving current are shown. Under 450nm-excitation from the LD source, the typical light emission spectra are shown in Fig. 5a. Moreover, before the saturation point, the luminance showed a linear relation to the output of the LD. The slope has a characteristic value for each phosphor sample and can be expressed as the change in the ratio between the velocity of N_{in} and the velocity of N_{out} . In Fig. 5b, before the saturation point, it was evident that the slope of the plot increased slightly as the intensity of the light source was increased by 50mA intervals from 200mA. The YAG of garnet series is structurally stable. It has excellent durability against temperature and light source. Therefore, it is assumed that the heat by the LD does not significantly affect the relaxation process. Here, since dN_{out}/dt is much larger than dN_{in}/dt , the accumulation of photons does not occur, so that N_{accum} converges to zero, and all absorbed photons are emitted. At 400 to 550mA, the slope of the actual data is slightly higher than the slope of the expected data. As the intensity of the LD exceeds 400mA, dN_{in}/dt becomes slightly larger than dN_{out}/dt , and the photons start accumulating. However, N_{accum} still converges to zero or less than N_{MAP} in this section. Above 550mA (saturation point), even if the current applied to the LD is derived and more photons excite the phosphor, the optical properties do not increase but rather drop sharply. Considering stability of YAG and CW mode, it may be caused by following reasons. First, it is most likely that the N_{in} is larger than the N_{MAP} and the efficiency drops because there is little difference between the expected data and actual data. Alternatively, it can be assumed that degradation occurred due to an internal/structural defect of phosphor in itself, since it is a result in the CW mode which does not consider the influence by the decay time.

For the measurement in pulsed mode, the data on the decay time of various phosphors were acquired at room temperature and atmospheric pressure, and the values represented half of the luminance as compared to the initial luminance. Based on this consideration, the decay time for the pulsed mode has been quoted from the literature values for the commercial YAG phosphor given that the present YAG sample was also of commercial level.³¹ As shown in Fig. 6, the

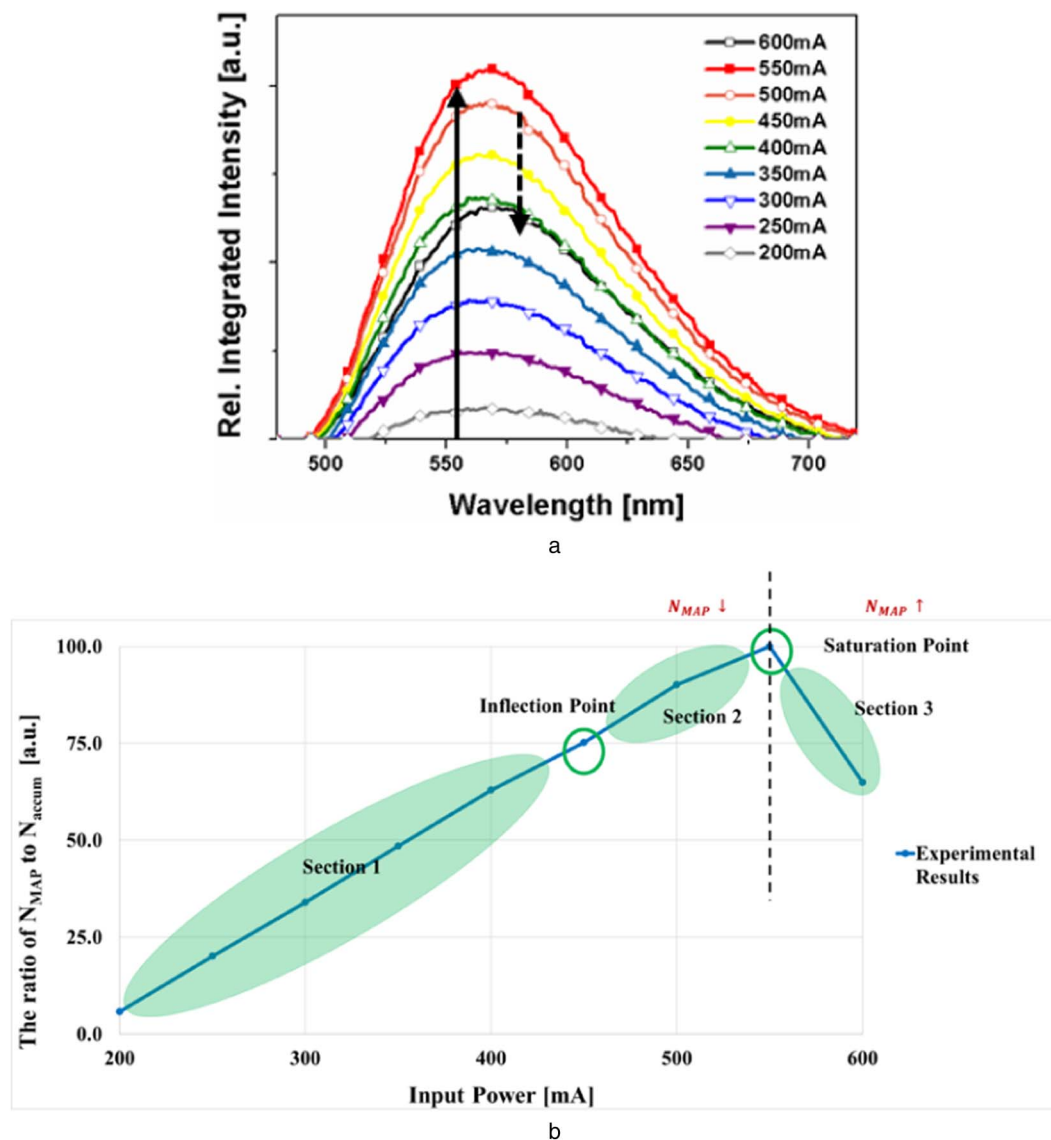


Figure 5. a. Photoluminescence spectra of $\text{Y}_3\text{Al}_5\text{O}_{12}:\text{Ce}^{3+}$ with increasing input power in continuous wave (CW) mode. b. Luminescence behavior of phosphor in continuous wave (CW) mode excitation.

results are slightly different from those of the CW mode, but tend to be the same overall, and the saturation point is also the same at 550mA. At 200 ~ 300mA, as in CW mode, dN_{out}/dt is much faster than dN_{in}/dt , so absorbed photons will be emitted and N_{accum} will converge to zero. At 300 ~ 350mA, dN_{out}/dt slightly decreases and the slope of actual data slightly increases than those of the expected values. However, since there is little difference between the two slopes, it can be assumed that N_{accum} converges to zero. After 350mA, the heat of the LD decreases the dN_{out}/dt in the section before the saturation point, and consequently dN_{in}/dt becomes larger than dN_{out}/dt . Therefore, N_{accum} begins to gradually develop from this interval, and N_{accum} converges to N_{MAP} . After the saturation point, crystal defects such as laser spots are not visible on the YAG surface, but the efficiency drops sharply when there is little difference from the expected curve. Through this, it is estimated that the measured YAG sample is highly efficient and stable for blue light, but the N_{MAP} is relatively small.

When the light source was irradiated at 200mA and 500mA (just before the saturation point), the YAG efficiency tended to change with temperature, and it was shown in Fig. 7. Table I summarizes

the results of increasing the temperature from room temperature to 423K by 25K for each output. Unlike the case of 200mA, which gradually degrades the optical properties as the temperature increases, the optical properties are rapidly deteriorated after 323K at 500mA. This suggests that when evaluating reliability at high power, it is impossible to absolutely exclude the effect on ambient temperature as well as the heat by non-radiative recombination. However, we also can control this effect by using peltier diode. More detailed data will be published.

Based on the above experimental observation, when a high flux of photons are irradiated to the phosphor, the certain point of a level where the light efficiency is sharply lowered occurs. The cause of this phenomenon can be largely limited to a luminescence saturation phenomenon or an internal defect caused by deterioration such as thermal quenching. Unlike the previous measurement, Fig. 8 shows the luminescent behavior of the phosphor sample, which was exposed to the photon radiation from the 650 mA-operating for LD 10 min. Then, the photon excitation is gradually decreased. As shown in Fig. 8, the photon output is even increased with decreasing photon excitation over the saturated range. It is decreased with the decreasing photon

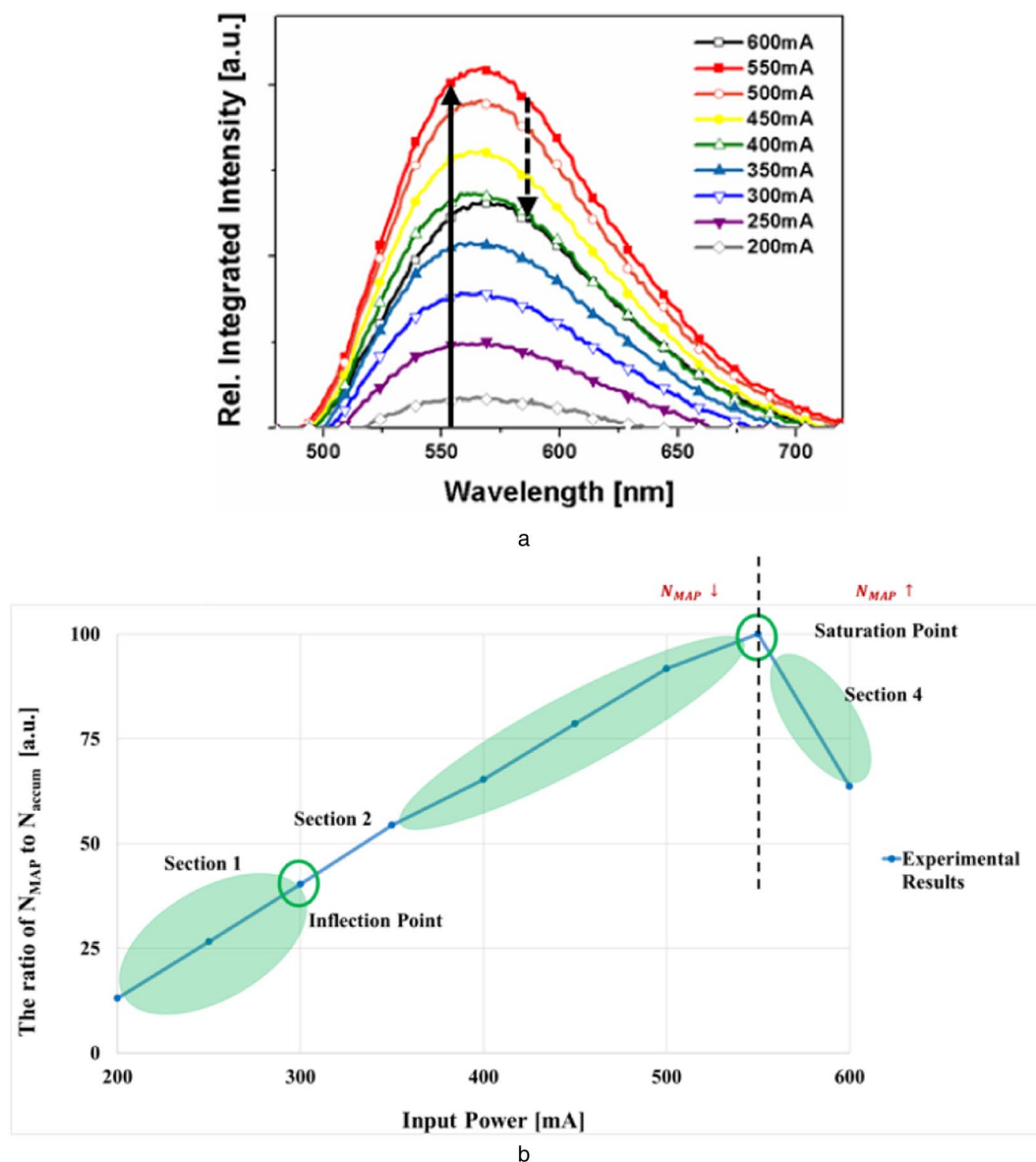


Figure 6. a. Photoluminescence spectra of $Y_3Al_5O_{12}:Ce^{3+}$ with increasing input power in pulsed mode. b. Luminescence behavior of phosphor in pulsed mode excitation.

excitation in normal range. Again, when it is raised over the saturation region of 650 mA through the saturation point of 550 mA, the optical characteristic decreases. However, the saturation point shows at the same level, which confirms the luminescence saturation phenomenon. However, hysteresis over the saturation region comes from the thermal effect.

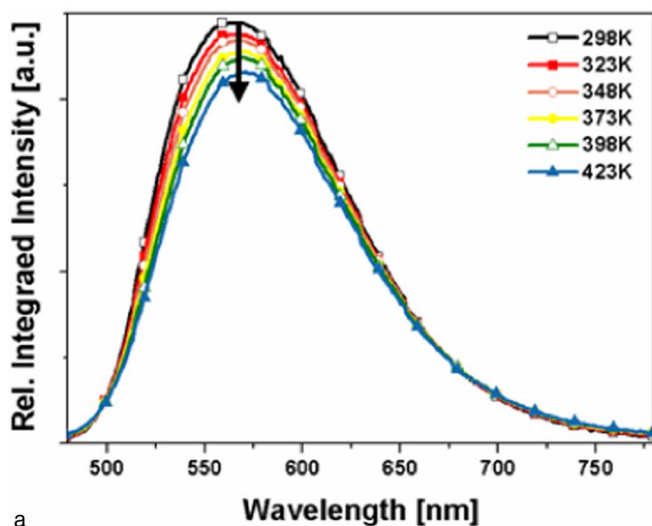
Finally, the simulation by data fitting is shown in Fig. 9, taking into account factors affecting luminescence saturation phenomenon and Eq. 1. In this graph, (a) represents the curve expected when photon-saturation does not occur (green line), and (b) and (c) represent the actual (blue line) and simulated (red line) data when photon-saturation occurs.

Conclusions

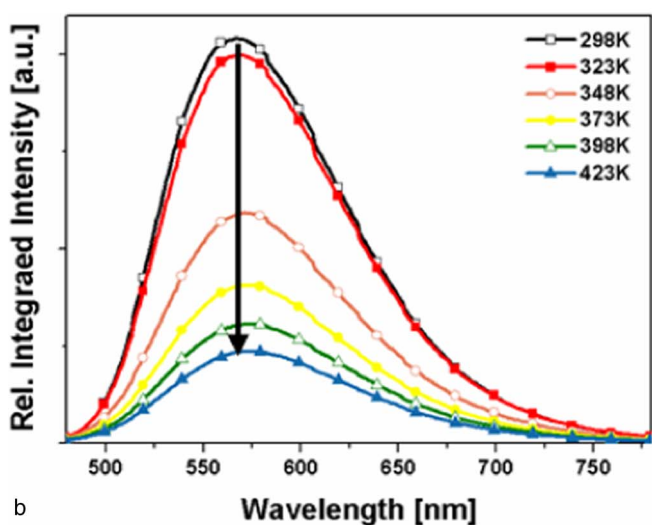
The optical durability and thermal stability of a solid-phase phosphor were evaluated simultaneously and at a high speed using the developed experimental equipment. The luminescence saturation phenomenon was defined and analyzed based on the experimental data. Luminescence saturation, i.e., the saturation brought about by the influence of different variables leading to an accumulation of photons, caused a change in the luminance and color coordinates of the phosphor. This, in turn, led to a reduction in the quantum efficiency of the phosphor. The conditions under which this phenomenon occurs must satisfy at least one of the following:

Table I. Relative luminance according to the temperature from 298K to 423K at 200mA-, and 500mA- driving LD excitation, respectively.

$Y_3Al_5O_{12}:Ce^{3+}$	298K	323K	348K	373K	398K	423K
200mA	100	97.5	96.0	93.4	91.9	88.9
500mA	100	95.7	57.2	39.6	30.1	23.4



a



b

Figure 7. a. Variation in luminance with the temperature from 298K to 423K at an output of 200mA. b. Variation in luminance with the temperature from 298K to 423K at an output of 500mA.

- (1) The probability of the activator ions going to the ground state must be lower than the probability of these ions going to the excited state. ($N_{accum} > N_{MAP}$)
- (2) The number of photons excited in the excited state is greater than the N_{MAP} of the phosphor. ($N_{in} > N_{MAP}$)

When these conditions are met, saturation occurs because the number of photons accumulated (N_{accum}) in the excited state exceeds the maximum acceptable number of photons (N_{MAP}) that can be accommodated. By creating a database of commercially available phosphor samples and adjusting the parameters by simulation, the reliability of the phosphor, which is based on its optical durability and thermal stability, can be predicted, and optimization and reliability evaluation of the sample can be expedited. We believe that this measurement scheme of the luminescence saturation shows the potential as a new indicator for reliability assessment of phosphors.

Acknowledgment

This research was supported by the Chung-Ang University Research Scholarship Grants in 2017.

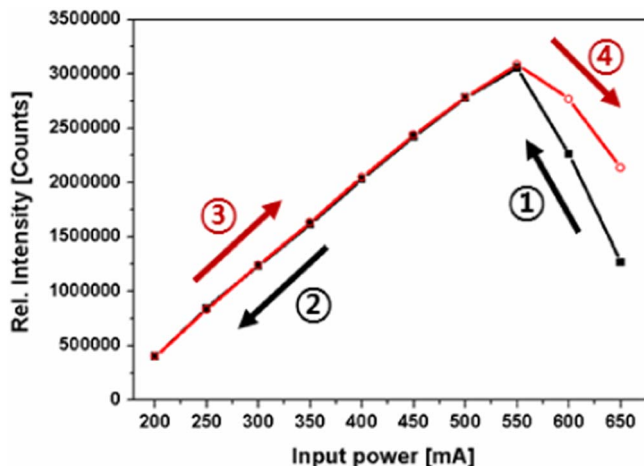


Figure 8. Luminescence behavior of the phosphor sample while decreasing the intensity of the light source down-to 200mA after the sample experienced the saturation behavior. Here, the phosphor sample are exposed to the photon radiation for 10 min and started to measure photon intensity at 650mA-operating LD excitation. Then successively, all the measurement has been done to low level of 200 mA-operating LD excitation. Again The output intensity is measured while increasing the input power.

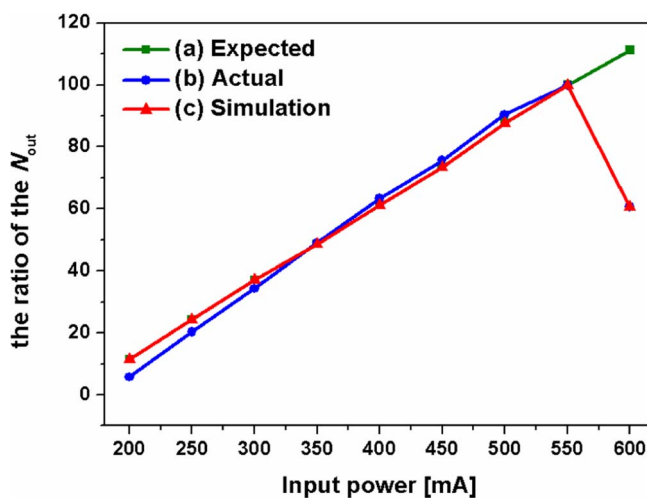


Figure 9. Experimental observation of luminescence behavior with and without luminescence saturation, and graph of N_{MAP} calculated using a proportional constant. (a) Expected curve when luminescence saturation does not occur (green line). (b) Actual line when luminescence saturation occurs (blue line). (c) Simulated line when luminescence saturation occurs (red line).

ORCID

Jae Soo Yoo <https://orcid.org/0000-0001-6194-3692>

References

1. J. J. Wierer, J. Y. Tsao, and D. S. Sizov, *physica status solidi (c)*, **11**(3–4), 674 (2014).
2. K. A. Denault, M. Cantore, S. Nakamura, S. P. DenBaars, and R. Seshadri, *AIP Advances*, **3**(7), 072107-1-7 (2013).
3. X. Luo, R. Hu, S. Liu, and K. Wang, *Progress in Energy and Combustion Science*, **56**, 1 (2016).
4. M. S. Jang, Y. H. Choi, S. Wu, T. G. Lim, and J. S. Yoo, *Journal of Information Display*, **17**(3), 117 (2016).
5. Z. Liu, T. Wei, E. Guo, X. Yi, L. Wang, J. Wang, G. Wang, Y. Shi, I. Ferguson, and J. Li, *Applied Physics Letters*, **99**(9), (2011).
6. M. Shatalov, A. Chitnis, P. Yadav, M. F. Hasan, J. Khan, V. Adivarahan, H. P. Maruska, W. H. Sun, and M. A. Khan, *Applied Physics Letters*, **86**(20), (2005).

7. A. A. Efremov, N. I. Bochkareva, R. I. Gorbunov, D. A. Lavrinovich, Y. T. Rebane, D. V. Tarkhin, and Y. G. Shreter, *Semiconductors*, **40**(5), 605 (2006).
8. Y. Im and J. Y. Lee, *Journal of Information Display*, **18**(3), 101 (2017).
9. H. F. Sijbom, J. J. Joos, L. I. D. J. Martin, K. Van den Eeckhout, D. Poelman, and P. F. Smet, *ECS Journal of Solid State Science and Technology*, **5**(1), R3040 (2015).
10. J. Piprek, *physica status solidi (a)*, **207**(10), 2217 (2010).
11. J. Iveland, L. Martinelli, J. Peretti, J. S. Speck, and C. Weisbuch, *Phys Rev Lett*, **110**(17), 177406 (2013).
12. J. S. Yoo, H. H. Lee, and P. Zory, *IEEE journal of quantum electronics*, **28**(3), 635 (1992).
13. N. J. Petersen, R. P. Nikolajsen, K. B. Mogensen, and J. P. Kutter, *Electrophoresis*, **25**(2), 253 (2004).
14. Y. C. Shen, G. O. Mueller, S. Watanabe, N. F. Gardner, A. Munkholm, and M. R. Krames, *Applied Physics Letters*, **91**(14), (2007).
15. M. F. Schubert, S. Chhahed, J. K. Kim, E. F. Schubert, D. D. Koleske, M. H. Crawford, S. R. Lee, A. J. Fischer, G. Thaler, and M. A. Banas, *Applied Physics Letters*, **91**(23), (2007).
16. P. Oliva, M. Carpinelli, B. Golosio, P. Delogu, M. Endrizzi, J. Park, I. Pogorelsky, V. Yakimenko, O. Williams, and J. Rosenzweig, *Applied Physics Letters*, **97**(13), (2010).
17. S. P. Singh, M. Kim, W. B. Park, J. W. Lee, and K. S. Sohn, *Inorg Chem*, **55**(20), 10310 (2016).
18. M. Kim, W. B. Park, B. Bang, C. H. Kim, and K.-S. Sohn, *Journal of the American Ceramic Society*, **100**(3), 1044 (2017).
19. J. W. Moon, B. G. Min, J. S. Kim, M. S. Jang, K. M. Ok, K.-Y. Han, and J. S. Yoo, *Optical Materials Express*, **6**(3), (2016).
20. I. Gregor, D. Patra, and J. Enderlein, *Chemphyschem*, **6**(1), 164 (2005).
21. J. J. Wierer, J. Y. Tsao, and D. S. Sizov, *Laser & Photonics Reviews*, **7**(6), 963 (2013).
22. O. B. Shchekin, P. J. Schmidt, F. Jin, N. Lawrence, K. J. Vampola, H. Bechtel, D. R. Chamberlin, R. Mueller-Mach, and G. O. Mueller, *physica status solidi (RRL) - Rapid Research Letters*, **10**(4), 310 (2016).
23. T. Jansen, D. Böhmisch, and T. Jüstel, *ECS Journal of Solid State Science and Technology*, **5**(6), R91 (2016).
24. R. B. Johnson, A. Lenef, J. Kelso, Y. Zheng, M. Tchoul, V. N. Mahajan, and S. Thibault, in "Current Developments in Lens Design and Optical Engineering XIV", **8841**, 1 (2013).
25. M. Kim, W. B. Park, B. Bang, C. H. Kim, and K.-S. Sohn, *Journal of Materials Chemistry C*, **3**(21), 5484 (2015).
26. X. He, X. Liu, R. Li, B. Yang, K. Yu, M. Zeng, and R. Yu, *Sci Rep*, **6**, 22238 (2016).
27. L. Wang, X. Zhang, Z. Hao, Y. Luo, L. Zhang, R. Zhong, and J. Zhang, *Journal of The Electrochemical Society*, **159**(4), F68 (2012).
28. H. Yang, D.-K. Lee, and Y.-S. Kim, *Materials Chemistry and Physics*, **114**(2-3), 665 (2009).
29. L. Chen, X. Chen, F. Liu, H. Chen, H. Wang, E. Zhao, Y. Jiang, T. S. Chan, C. H. Wang, W. Zhang, Y. Wang, and S. Chen, *Sci Rep*, **5**, 11514 (2015).
30. X. W. Xiaodan Wang, H. M. Hongmin Mao, C. M. Chunlan Ma, J. X. Jun Xu, and X. Z. Xionghui Zeng, *Chinese Optics Letters*, **10**(7), 071601 (2012).
31. G. He, L. Mei, L. Wang, G. Liu, and J. Li, *Crystal Growth & Design*, **11**(12), 5355 (2011).